Thunderstorm characteristics of importance to wind engineering Part I: Temporal scales and turbulence

Franklin T. Lombardo[a*], Douglas A. Smith[b], John L. Schroeder[b], Kishor C. Mehta[b]

[a] *National Institute of Standards and Technology, Gaithersburg, Maryland 20899, MS 8611*

[b] *Wind Science and Engineering Research Center, Texas Tech University, Lubbock, Texas 79414*

Abstract

The idea that "wind is wind" allows statistics for wind and pressure collected in wind tunnels to be used in wind load standards. Statistics collected in wind tunnels are based on inherently stationary data and verified with field data that is stationary in the boundary layer (SBL). Some of the most extreme and important events for wind loading (e.g. thunderstorms) display non-stationary wind and pressure characteristics. Thunderstorms are therefore assumed to have the same properties as the SBL, although previous studies have shown differences. Wind data from thunderstorms, some of which displayed rapid wind speed increases (i.e. "ramp-up") were collected at Texas Tech University and from field campaigns. General characteristics of the ramp-up events are detailed. Time scales and turbulence are compared with SBL data. Analysis revealed averaging times of 15 s - 60 s can be used in SBL comparison. Shorter time scales than typically used in wind engineering were found for ramp-up events. Ramp-up turbulence in the frequency domain was similar to the SBL and turbulence intensities fell within the range of the SBL at 15 s - 60 s averaging times.

Keywords: **Thunderstorm; Non-Stationary; Turbulence; Time Scale**

1. Introduction

The engineering properties of wind, no matter the source, are homogenous. This is the fundamental assumption of current wind engineering practice. The idea that "wind is wind" allows statistics for wind and wind-induced pressure currently collected in wind tunnels to be used in wind load standards. Statistics collected in wind tunnels are based on data that inherently display steady mean and variance, known as *stationary* data. Wind tunnel results are validated with full-scale data that is stationary within the boundary layer (SBL) and over durations associated with the spectral gap (10 min to 120 min, Stull, 1988). Contrarily, thunderstorms, one of the most extreme and hence important events for wind loading, typically display wind

[*] Corresponding Author: Tel: (301) 975-5983
E-Mail Addresses: franklin.lombardo@nist.gov (FT Lombardo), doug.smith@ttu.edu (DA Smith), john.schroeder@ttu.edu (JL Schroeder), kishor.mehta@ttu.edu (KC Mehta)

and wind-induced pressure of unsteady mean and variance, and occur over shorter time scales associated with the spectral gap. These events are referred to as *non-stationary*. Non-stationary events such as thunderstorms are therefore assumed to have the same statistical and physical properties as stationary events in wind load standards. These assumptions have been shown to be questionable in some cases (Fujita, 1985; Kim and Hangan, 2007; Holmes et al., 2008). As a result, Orwig and Schroeder (2007) as well as Choi and Hidayat (2002) state that the wind load standard is not adequately suited for thunderstorm events. Figure 1 shows an example of a stationary wind speed record and a non-stationary wind speed record generated by a thunderstorm.

Thunderstorm wind and pressure data have long been challenging to the wind engineering community due to their transient (i.e., non-stationary, short temporal scale) characteristics. These characteristics render traditional correlation, spectral analysis and statistical techniques inappropriate. This is especially true in "ramp-up" thunderstorm events lasting over short time periods as shown in Figure 1. Calculation of wind engineering statistics (e.g., turbulence intensity, gust factor) used in wind load standards are based on stationary wind data with longer temporal scales than most ramp-up events. Due to these transient characteristics and lack of available field data (Kwon and Kareem, 2009), meaningful comparisons with non-stationary events are unwieldy.

In addition to its transient characteristics, thunderstorm flow shows physical differences from the SBL that may affect wind characteristics and wind-induced pressures. Thunderstorm flow has been hypothesized to have lower turbulence and higher lateral correlations than SBL flow (Holmes et al., 2008). Lower turbulence and higher correlations may have implications for pressure distribution on low-rise buildings. Significant low frequency content found in thunderstorms (Holmes et al., 2008; Chen and Letchford, 2007) may affect long-span structures such as transmission lines and suspension bridges (Li, 2000). Rapid changes in wind speed may also hide frequency information important for structural response (Juhasova, 1997) as this information is poorly understood for thunderstorm events (Kim and Hangan, 2007).

Full-scale thunderstorm wind data was collected at Texas Tech University and from field campaigns from 2003 to 2010. A listing of ramp-up events that were collected is found in Table 1. Due to the difficult nature of thunderstorm charactersitics, a number of studies (Holmes et al., 2008; Chen and Letchford, 2005) have assumed that instead of a constant mean wind speed over the course of the record, non-stationary data has a time varying mean wind speed. This time-varying mean wind speed at some averaging time is then compared with the constant mean wind speed of the stationary data in the computation of wind engineering parameters. The respective means are then subtracted from the original record to generate "residual turbulence". The values of both time-varying mean and residual turbulence will be used throughout this paper to compare thunderstorm wind data to that of the SBL. The averaging times used in the computation of time-varying means are shown in Table 2.

The data was collected to greatly increase the number of available thunderstorm data sets for research purposes. The time-varying mean and residual turbulence quantities of the thunderstorm wind data were used to make sound comparisions with SBL wind data. These comparisons enabled further information on the statistical and physical differences from the SBL, and subsequent identification of thunderstorm characteristics of potential importance to wind engineering. Temporal and turbulence properties are the characteristics discussed in this paper.

2. Data Instrumentation and Collection

2.1 Site Characteristics/Instrumentation

Nearly all of the wind data analyzed for this work was collected at the Wind Engineering Research Field Laboratory (WERFL) at Texas Tech University. The original WERFL site included a 50 m tower with meteorological instrumentation at five levels. The original WERFL site was generally considered to be in "open" exposure (Levitan and Mehta, 1992), representative of "Exposure C" in ASCE (2010). In fact the mean roughness length value collected over 693 15-min SBL runs (which will be used over the course of this paper) using the profile method at the original site was 0.015 m (0.049 ft), near the "typical" values prescribed in ASCE (2010) for Exposure C.

The WERFL site was moved to a location 15 km west of Lubbock in 2006 known as Reese Center. Reese Center, site of a decommissioned Air Force Base, is also in "open" terrain, but may be more representative of "Exposure D", or marine exposure, as noted in Vega (2008). While the 50 m (160 ft) tower remained at the original site, a 200 m (656 ft) tower exists at Reese Center with meteorological instrumentation at ten levels. The anemometry used for wind speed and direction measurements at both sites was RM Young Gill 27005T u-v-w anemometers (Lombardo, 2009).

The May 14, 2008 event was collected by "StickNet" a ruggedized, rapidly portable instrumentation system (Schroeder et al., 2009) with anemometery at around 2.25 m (7 ft) above the surface. Although terrain characteristics were unkown, common practice is to site the anemometer in relatively open terrain conditions.

Due to the relatively small number of data points in the thunderstorm/ramp-up cases, it was difficult to make exact roughness/terrain comparisons, and it is likely very difficult to do so. Therefore, all data, when used in comparison, was assumed to be in open exposure, classified as "Exposure C" in ASCE (2010).

2.2 Thunderstorm/"Ramp-Up" Identification and Definition

Thunderstorm identification was typically performed in these steps:

1) Identifying thunderstorm reports in archived Automated Surface Observing System (ASOS) reports

2) Verifying information in 1) using archived radar images located at the link (http://locust.mmm.ucar.edu/case-selection)

3) Due to spatial differences in 1), particular runs in the WERFL database for the time frame identified in both the previous two steps were checked for:

    a. Wind speed increases

    b. Wind direction changes

    c. Pressure/air density increases and/or decreases

If the run met all these criteria, the run was labeled as a thunderstorm. This information was then additionally checked with archived surface wind observations from the link above or from the West Texas Mesonet (Schroeder et al., 2005). A secondary check of radar data from periods of peak thunderstorm activity was also performed to collect additional events that may not have been recorded in ASOS. More recent events occurred while research presented in this paper was ongoing, so the occurrence of thunderstorm generated winds was inferred by immediately checking the recorded data from the WERFL site, radar imagery and other observation tools (see Section 2.1).

In addition, a number of thunderstorm records were found to have an extremely rapid increase and subsequent decrease in wind speed over a short period of time (5 min or less). These were denoted as *ramp-up* events as described in Section 1 and also defined in Fujita (1985), and will be analyzed as such over the course of this paper. Examples of these types of events are shown in Figures 1 and 2. Table 1 shows a summary of the ramp-up cases studied in this paper. The temporal scale (Section 3.3) and peak wind speed values denote near surface measurements. All near surface measurements were collected from approximately 10 m (33 ft) with the exception of May 14, 2008 which was collected at approximately 2.25 m (7 ft) and June 4, 2009 at 17 m (55 ft).

3. Thunderstorm/Ramp-Up Wind Characteristics

3.1 General Characteristics

The time histories of eight ramp-up cases that were collected are shown in Figure 2. The ramp-up periods occur over a number of relatively short time intervals, discussed in Section 3.3, and fit the basic definition given in Section 2.2. Another interesting observation is that none of the cases follow the traditional time history model for a downburst/microburst event as observed in the 1983 Andrews AFB microburst (Fujita, 1985) and modeled in a number of publications such as Holmes and Oliver (2000). These differences may be due to the fact the downburst may not have passed directly over the measuring point (Holmes and Oliver, 2000) however the wind directions over the time of the ramp-up periods are relatively constant (Lombardo, 2009). Regardless, the secondary, lesser wind speed peak shown occasionally in observation and duplicated in

other studies is practically of no consequence to wind engineering design due to its low value in comparison to the peak wind speed, and hence, potential peak wind load of the entire event. As the type of thunderstorm is listed in Table 1 and mentioned throughout this paper as a possible important parameter in wind engineering, this property should be further studied as no two thunderstorm time histories are exactly alike. Generation mechansims for thunderstorm wind producers are discussed in a meteorological context in Wakimoto (2001) and an engineering context in Lombardo (2009).

3.2 Thunderstorm Periodicity

Holmes et al. (2008) and Chen and Letchford (2007) noted the presence of significant low-frequency wind components that reflected the main flow features of a supercell thunderstorm event. It was also noted that the period of these fluctuations appeared to be around 100 s. Similar periods have also been noted in wind tunnel simulations (Kim and Hangan, 2007). However, SBL winds show similar dominant periods in a number of different engineering models of turbulence. Fujita (1986) and Skinner et al. (2010) note that downdrafts from an non-supercell and a supercell thunderstorm respectively appear to have some pulsating or periodic component and both note the presence of three "surges" produced from the parent thunderstorm.

Three non ramp-up records collected at the Reese site visually showed evidence of periodic wind speed components (Figure 3). The computation of typical wind engineering parameters such as turbulence intensity over a 5 min period for a relatively "stationary" case in Figure 3a (~ 0.18) is much higher than the expected 5 min values at Reese Center (0.12-0.13) shown in Vega (2008). The three 5 min thunderstorm time histories were linearly detrended and compared in the frequency domain with 124 randomly selected 5 min SBL time histories which were also detrended. The time histories were converted into the frequency domain using Welch's power spectral density with no overlap due to the relatively short record length.

Figure 4 shows some interesting results. Although the prominent frequency for both the thunderstorm and SBL events appear to be around the same values (~0.01 Hz), the thunderstorm energy appears to be more "peaked" and contain higher energy than the SBL events. This property may also indicate a larger

longitudinal “eddy size” using traditional statistical methods. However due to the fact that the thunderstorm energy is averaged over only three cases and the large variance in the values of energy in 124 SBL cases (Figure 4), especially those at lower frequencies (Simiu and Scanlan, 1986), it is difficult to determine if any actual differences exist in the flow characteristics of these particular thunderstorm events. The higher frequency representation of thunderstorm ramp-up events compared with traditional SBL models are shown in Section 3.4.

The addition of severe thunderstorm field projects such as VORTEX2 should help engineers and scientists to more completely understand the thunderstorm phenomena, and the wind characteristics that it produces. Two such cases collected in the 2009 segment of the VORTEX2 project also displayed interesting characteristics including thunderstorm periodicities, although at relatively low wind speeds and frequency components. In Figure 5, it is evident that there are periodic components for both records shown. These periodicites are approximately 30 s in Figure 5 (left) and 300 s in Figure 5 (right). Low frequency components (0.01 Hz to 0.05 Hz), especially those shown in Figure 5 (left) are close to the natural frequencies of some long-span bridges across the world (Simiu and Miyata, 2006). These periodicities are likely more related to convective processes than mechanical mixing.

3.3 Thunderstorm Temporal Scales

As discussed above, thunderstorms are typically of small temporal scales (i.e. < 5 min). As most wind records are collected over longer durations, thunderstorm winds may only be contained within a portion of that record. It is important to then extract information only relevant to the thunderstorm event and to determine what time scale is important for thunderstorm winds (Choi and Hidayat, 2002). It has been visually shown (Figure 6) and noted in other studies (Holmes et al., 2008) that when a time-varying mean is applied to the data, the remaining residual turbulence shows areas of differing variability. Wind engineering parameters using data of differing variability would cause these values to be improperly represented. In fact, a time evolving turbulence has been noted for SBL events as well (Ewing et al., 2005). A segmentation algorithm explained in the following section can be used to separate areas of differing variability.

3.3.1 Segmentation Algorithm

Using the ramp-up cases and 34 other non ramp-up thunderstorm events, the residual turbulence data was extracted (Equation 1) using an averaging time of 17 s The 17 s averaging time was used to ensure the mean of the residual turbulence would be approximately zero (see Section 3.3.2) and only changes in variance would be tested. The definition of residual turbulence is as shown:

$$U' = U - \widetilde{U}_t \tag{1}$$

where U is the original time history of the record and $\widetilde{U}_t$ is the time-varying mean using some averaging time denoted as t.

Each time history was then analyzed for potential changes in variance using the reverse arrangement test (NIST, 2006) and runs test (Bendat and Piersol, 2000) with a significance level of 0.01. The non-stationary time histories (900 s and 1500 s were broken up into 225 segments and tested 18 segments at a time to avoid violating normal distribution assumptions. If segments 1-18 were deemed to be statistically stationary by both tests mentioned above, the algorithm moved to analyze segments 1-19, 1-20 and so on until the test revealed statistical non-stationarity in one or both of the tests. This occurrence of statistical non-stationarity will be otherwise known as a "change point". The change point is marked at the specific time of this non-stationarity within the algorithm and the algorithm is then started anew at that particular point in time. The algorithm continues to run in the same manner until it reaches the end of the record.

This algorithm was then run 500 times with the first run starting at the first data point and the final run starting at data point number 500 in the same manner as discussed in the previous paragraph. A probability density function was then estimated for the distribution of change point locations over the time histories for the 500 runs to determine optimum change point locations. Definitive peaks in the density function were recorded and used as change points. Further visual inspection was able to sharpen the change-points.

Once two change-points (or one change-point and the beginning or end of the record) were revealed between the maximum wind speed in the record (Figure 7), the stationary residual turbulence segment, U'_{seg}, and the

time-varying mean segment, $\widetilde{U}_{t,seg}$ contained from that portion of the record were used for wind engineering parameterization (i.e. turbulence intensity, gust factor) in the following sections.

In addition to the 17 s averaging time, 19 other averaging times were then used to calculate U'_{seg} and $\widetilde{U}_{t,seg}$ for the statistically stationary residual turbulence segment that contained that maximum wind speed using the 17 s averaging time. As wavelet decomposition was used for the averaging time calculations, averaging times were tied to powers of two and the sampling frequency of the data (Chen and Letchford, 2005). The 20 averaging times used are shown in Table 2. Simple moving averages have shown to compare well with wavelet generated moving averages (Lombardo, 2009).

3.3.2 Mean Residual Turbulence

After the time-varying mean was extracted out of the data and the stationary segment was identified, the mean of the residual turbulence of that stationary segment was calculated. In equation form:

$$\overline{U'_{seg}} \tag{2}$$

Where again U'_{seg} is the residual turbulence of the stationary segment containing the peak wind speed as computed in Equation 1 for one of the 20 averaging times used over that segment. If the time-varying mean effectively captures the non-stationarities in the original wind speed time history that contain the peak wind speed, the mean of the residual turbulence should be around zero. An attempt therefore to both minimize non-stationary characteristics and maximize the averaging time to retain as much information as possible in the residual turbulence was carried out. Figure 8 shows the mean residual turbulence of 42 thunderstorm events with the 8 ramp-up events indicated in gray.

Up to 34 s most of the $\overline{U'_{seg}}$ values for all thunderstorm events, including ramp-up events are near zero. A zero $\overline{U'_{seg}}$ value implies that averaging times around 34 s used on non-stationary wind speed time histories may be used to calculate wind engineering parameters, as will be talked about in the following sections in this paper. All ramp-up events appear to converge to zero around this time as well. Testing inferences on a zero mean using both parametric and non-parametric methods for this data revealed that the tests on a zero mean failed

after the 68 s averaging time with the exception of averaging times around 3 s - 4 s The cause of rejection of zero mean at these averaging times is likely due to chance as the values were approximately 0.007 and 0.008 respectively. Nevertheless, this analysis on residual turbulence again suggests that the averaging time range found by Holmes et al. (2008) is reasonable and from events in this study is probably appropriate for averaging times 15 s – 60 s.

3.3.3 Residual Turbulence Temporal Scales

After the algorithm described in Section 3.3.1 was carried out, the stationary segment lengths that contained the peak wind speed were recorded. A wide variance is exhibited among stationary time segments, and it is difficult if not impossible to determine a "mean" stationary segment length for blanket use in analysis. The average stationary segment length of all thunderstorm events was approximately 270 s with a standard deviation of approximately 186 s. For only ramp-up events, the mean segment length was 165 s with a standard deviation of 80 s. The minimum segment length was approximately 70 s.

The time scales found above correspond fairly well to what has been noted in the literature. Choi and Hidayat (2002) and Kwon and Kareem (2009) noted that high wind speeds lasted about 120 s – 180 s in a supercell thunderstorm event. The well known Andrews AFB downburst had a ramp-up period of approximately 90 s - 100 s. Holmes et al. (2008) noted that high amplitude wind fluctuations in a thunderstorm event occurred over an approximately 100 s duration. In an analysis of non-stationary events, Duranona et al. (2007) found strong wind speed increase ranged anywhere from 2 min - 6 min with decreases including an additional 1.5 min - 8 min. Using records in Brazil, Ponte and Riera (2010) found mean temporal scales of 380 s and a standard deviation of 164 s measuring from the "beginning" of the event until the wind speed reaches its maximum value. Similar times have also been noted in meteorological studies of microbursts (Wakimoto, 2001).

Holmes et al. (2008) states that "An obvious conclusion is that codification based on 10 min or hourly means is not appropriate for locations where thunderstorm downdrafts are the dominant strong wind event". Based on previous research and the information found in this study, durations of time typically associated with the spectral gap are *not* appropriate for areas in which thunderstorms dominate the extreme wind climate. More

appropriate time periods for extreme events are likely around 60 s to 240 s. Proper time periods are likely to be determined on a case by case basis and it has been shown by the algorithm described in Section 3.3.1 that the time segment of interest may be associated with the ramp-up portion of the event (Figure 7).

3.4 Turbulence

3.4.1 Surface Roughness/Power Spectral Density

Much discussion has been devoted to the short fetch of thunderstorm winds due to their generation mechanisms, which, in principal should render the turbulent properties of thunderstorms different than those of the SBL (Holmes et al., 2008; Ponte and Riera, 2007; Chen and Letchford, 2007; Choi, 2004). Short duration, rapid increases and subsequent decreases in wind speed as shown in Figure 2 are likely indicative of convectively generated winds that have had little or no contact with the surface. However, Ponte and Riera (2007) note that an analysis of thunderstorm wind records revealed the majority of the energy within the band noted for synoptic wind events. In some modeling studies (Chay et al., 2008) and in field work (Fujita, 1981), it has been noted or assumed that the maximum wind speeds typically occur at distances up to 1.5 km (~ 1 mi) away from the parent downdraft. Hjemfelt (1988) noted that the highest wind speed typically occurred around one downdraft jet diameter from its point of impact. From a maximum wind speed (design) standpoint this gives the wind, especially near the surface, time to develop characteristics defined by surface roughness. Similar distance of the maximum wind speed from downdraft impact has also been noted in wind tunnel simulations (Mason et al., 2005, Wood et al., 2001). In addition, surface roughness may have some effect on air parcels before they become ingested into a thunderstorm updraft and subsequently end up in a downdraft. Other studies have shown that the fluctuating wind component in non-stationary events is similar to that in boundary layer winds (Kwon and Kareem, 2009, Holmes et al. 2008). Fujita (1981) suggested that the maximum expected winds from a downburst will be over larger scales (~ 100 m) than most small scale structures such as low-rise buildings, indicating similarities to SBL winds.

The residual turbulence generated from Section 3.3 was used in the estimation of power spectral density. The residual turbulence of the stationary segments used was extracted using a moving average of 34 s (Section 3.3.2). Due to the extraction of low frequency content using the moving average, frequencies lower than 25 s^{-1}

(0.04 Hz), were disregarded from the analysis. Frequencies above 1 s^{-1} (1 Hz) were also left out of the analysis due to response and noise issues of both the uvw and sonic anemometers. In addition, the shortest segment length was 70 s. Due to the loss of reliable frequency information as the segment analyzed becomes shorter, it is usually good practice to use segments nearly 3 times the length of the maximum period being analyzed (Stull, 1988). Since only one event was below this threshold, all spectral energy information was assumed reliable.

Spectral energy information was normalized by frequency and variance of the record and compared with three different spectra: The Harris-Von Karman spectrum, the Florida State University (FSU) perturbed terrain and the Kaimal neutral stability spectra (Holmes, 2001; Masters, 2004). The Harris – Von Karman spectra:

$$\frac{fS_u(f)}{\sigma_u^2} = \frac{4n}{\left[(1+70.8n^2)^{5/6}\right]} \tag{3}$$

where *n* typically equals:

$$n = \frac{fL}{U} \tag{4}$$

In the traditional case *f* is the frequency, *L* is the longitudinal integral scale and *U* is the mean wind speed. In this case *n* equals:

$$n = \frac{fL_u}{\bar{\bar{U}}} \tag{5}$$

Where L_u is the mean integral scale of the thunderstorm ramp-up events using the autocorrelation method (Simiu and Scanlan, 1986) at the 34 s averaging time. This L_u value was 60 m (220 ft). $\bar{\bar{U}}$ is the overall mean of the time-varying mean wind speeds in the segment containing the peak wind speed for all thunderstorm events.

The FSU perturbed terrain spectrum:

$$\frac{fS_u(f)}{\sigma_u^2} = \frac{40.42n}{\left[(1+60.62n)^{5/3}\right]} \quad (6)$$

Where *n* is the reduced frequency and is calculated as:

$$n = \frac{fz}{\bar{\bar{U}}} \quad (7)$$

where *z* is the height of measurement (10 m). This value was also used in the computation of the Kaimal spectrum:

$$\frac{fS_u(f)}{\sigma_u^2} = \frac{33.33n}{\left[(1+50n)^{5/3}\right]} \quad (8)$$

The spectra that were used in this case are normalized by the variance. Normalization by variance was done due to the difficulty in computing friction velocity, used in some formulations of spectral energy, due the original nonstationarity of record. The Welch Power Spectral Density method was used to normalize observed turbulence with no overlap. In addition, since the stationary residual turbulence segments varied in length, the spectral energy was binned over a range of frequencies and an average frequency within each binned range was used in computation of a composite spectrum for Figure 9.

In Figure 9 it is shown that energy decay using the three spectra are fairly robust when considering higher frequencies of ramp-up high frequency turbulence (> .05 Hz). The Harris – Von Karman spectrum does show the most accurate comparison of both thunderstorm and ramp-up spectral energies, likely due to the use of the lower integral scale (~ 60 m) as stated previous. This integral scale value is due to the removal of low frequency energy using the moving average calculations. A higher integral scale, as used in ASCE (2010) for all terrain exposures, would have caused the SBL models to show lower energies at the frequencies studied.

3.4.2 Wavelet/Alternative Analysis of Power Spectral Density

Another method to analyze information in the frequency domain is through the use of wavelets. Wavelets are beneficial for non-stationary records due the local amplitude differences of the wavelet, which, unlike the

Fourier transform, enables wavelets to detect frequency information at specific areas of interest (Gurley et al., 2003). In previous studies, wavelet analysis for non-stationary extreme wind events exhibited a similar turbulent structure to that expected in boundary layer flow and a significant portion of the energy was contained at low frequencies (Duranona et al. 2007). A Daubechies wavelet of order 4 was chosen in this case due its use in other wind engineering applications (Gurley et al., 2003; Chen and Letchford, 2005), and its ability to reduce "shark fins", reconstruct the original signal, and provide compact support (Percival and Walden, 2000). For further information on the mathematics of the Daubechies 4 wavelet, please consult Percival and Walden (2000). However, the choice of wavelet function is not critical, since quantitative results will be the same (Duranona et al. 2007).

Two examples of evolutionary frequency processes for ramp-up events are shown in Figures 10 and 11. The spectral energy was normalized by the 34 s time-varying mean wind speed to lessen the effects of higher energy from higher wind speeds. The ramp-up in wind speed in Figure 10 basically occurs from the start of the record to 100 s into the record. Over this period the majority of the spectral energy is at very low frequencies (< 0.1 Hz). In fact, over 99% of the energy contained over the ramp-up period was less than 1 Hz, which is below the natural frequency of most structures. In the second ramp-up event (Figure 11) at a height of 17 m (55 ft), which produced the highest wind speeds of any ramp-up case collected, the majority of energy was again at low frequencies. However there does appear to be a short "burst" of energy around 520 s at a frequency of approximately 0.2 Hz. Wang and Kareem (2005) noticed similar energies using the Hilbert Huang transform present in a supercell thunderstorm. This study and others have shown that in general, wind generated from thunderstorms is a low frequency process and possibly contain higher energy than the SBL at low frequencies. Whether thunderstorms present additional energy at high frequencies as opposed to SBL events remains to been seen and will be discussed in the next section.

3.4.3 Turbulence Intensity (TI)

As in other wind engineering parameters, the calculations of turbulence intensity for thunderstorm events have shown contradicting results. Duranona et al. (2007) found turbulence intensities for ramp-up wind events

decreased with height, similar to SBL flow. The authors also note a slight shift to lower turbulence intensity values due to the rapid increase in wind speed without the required time for turbulence production. Choi (2000) found higher turbulence intensities in tropical thunderstorms using a 1 hr mean value. The turbulence intensity values calculated in Holmes et al. (2008), Chen and Letchford (2005, 2007) for a supercell thunderstorm event are lower than the turbulence intensity values specified in ASCE 7 using moving average values around the ranges given in Section 3.3.2. However, when using approximately a 30 s time-varying mean on 693 SBL cases, the effective turbulence intensity (Equation 9), on average is reduced by 30 % from 0.185 to 0.129 (Figure 12). Figure 12 may also be a passive indicator of the spectral gap, as turbulence intensities remain similar at averaging times of 273 s and above. Turbulence intensities calculated using 2 min unmodified SBL data in Orwig and Schroeder (2007) were actually lower than the time-varying mean turbulence intensities of Holmes et al. (2008) for the same roughness regime. This suggests that the low turbulence intensity values deduced from strong thunderstorm observations in previous studies were likely a product of the averaging scheme used and not a characteristic of the inherent flow. However, since moving average techniques do lower TI values, it would be beneficial to reduce or supply a range of turbulence intensity values due to the removal of low frequency data if ever adopted into building codes or standards.

In this work, turbulence intensities of ramp-up events were calculated at a number of averaging times similar to the mean residual turbulence in Section 3.3.2. The turbulence intensity equation used in this work:

$$TI = {\sigma_{U'seg}}\Big/{\overline{\widetilde{U}_{t,seg}}} \tag{9}$$

where $\sigma_{U'seg}$ is the standard deviation of the stationary segment and $\overline{\widetilde{U}_{t,seg}}$ is the mean of the time-varying mean of the stationary segment. This value will result in an average turbulence intensity value over the entire stationary segment.

The 8 ramp-up events were compared with the 693 SBL events over 10 averaging times (odd numbers in Table 2). In addition to the 900 s (15 min) SBL records, a random 100 s segment was chosen from each of the 693 SBL records to compare with the average segment length of the ramp-up events (~ 165 s). The mean

wind speed over that 100 s period was used in the computation of turbulence intensity to make similar comparisons with ramp-up events. Shown in Figure 13 is each of the individual ramp-up events with the ranges of turbulence intensity for both the 900 s and 100 s segments as well as the 10^{th} and 90^{th} percentiles of SBL TI. Within the 15 s to 60 s averaging times prescribed in Section 3.3.2, all ramp-up cases fall within the bounds of the 100 s ranges with most falling within the 900 s range and the 90^{th} percentile of the 100 s range. The ramp-up events falling inside the bounds of turbulence intensity at these averaging times further reinforce the use of the particular averaging times outlined in Section 3.3.2 for comparisons with the SBL, as TI values are similar. At averaging times greater than 60 s, as expected, the non-stationary properties of most ramp-up events are evident. The black dot represents an observation from "StickNet" taken at a height of 2.25 m (7 ft). Higher turbulence is inherent in observations at this height; however these values still fall within the 100 s TI bounds.

Although within the bounds of the SBL, in general, some TI observations in ramp-up events fall higher than the majority of their SBL counterparts at averaging times less than 60 s as noted by the 10^{th} and 90^{th} percentile calculations. These higher TI observations, although in "open" exposure as stated previous, took place in an area with generally smoother terrain than those in the SBL. This could be due to extremely small scale ramp-up events (~10 s or less) that were not captured by the algorithm and are possibly incorporating another turbulence regime at higher wind speeds (Chen and Letchford, 2005). The extremely rapid nature of these gusts also may lead to higher turbulence due to the time-varying means at higher averaging times not being able to respond to the rapid change in wind speed. Again, the time segment of interest may be associated with the ramp-up portion of the event (Figure 7). Another idea is that an expected value of TI from these events may actually be higher than of that SBL owing to some contribution from convective processes. As uvw anemometers with response issues were used in the study, turbulence at higher frequencies is difficult to quantify. High resolution, quality controlled sonic anemometers would be best suited for a study of this type. Nevertheless, using 39 thunderstorm events, the median values of TI were statistically equivalent to TI values of the SBL at averaging times greater than 34 s (Lombardo, 2009).

4. Conclusions

For wind engineering purposes, thunderstorms have traditionally been difficult to analyze and therefore have been prohibitive for comparisons with wind tunnel and SBL data. Due to this difficulty, a number of thunderstorm/ramp-up events were collected, described and analyzed in this paper. The objective of the work was to gain valuable insight on their characteristics and subsequent importance in wind engineering.

General characteristics of ramp-up events show the period of ramp-up is between 10 s -200 s and no secondary peak is noted as in previous publications and models. Thunderstorm type needs to be further studied as general characteristics differed from event to event.

Significant low frequency components were identified in some thunderstorm events with periods of approximately 100 s. Due to the higher energy associated with these events, it may suggest larger eddy sizes for events similar to the ones in this paper. Further field studies such as VORTEX2 may help enlighten these issues, especially for long-span structures vulnerable to low frequency processes.

A separation algorithm was employed to identify areas of constant variability for wind engineering parameterization. This was done be subtracting a time-varying mean from the thunderstorm data and obtaining a residual turbulence quantity. Using the segmentation algorithm it was discovered that 15 s - 60 s averaging times are acceptable for comparisons with SBL data and ramp-up events were associated with a 165 s average temporal scale. This 165 s temporal scale is much shorter than the temporal scales used in wind load standards and SBL calculations. Therefore, temporal scales currently used are not appropriate in thunderstorm prone regions. A suggestion is the use of temporal scales ranging from 60 s - 240 s. In addition, the temporal scale may be comparable to the ramp-up portion of the event.

Using the segmented residual turbulence, ramp-up turbulence was found to be similar to SBL models in the frequency domain for frequencies ranging from 0.05 Hz to 1.0 Hz. Wavelet analysis also suggests relatively low frequency turbulence similar to that of the SBL. Lower turbulence intensity values found in previous studies were likely solely a function of averaging time as SBL turbulence intensity values were reduced, on average, by 30% using a 34 s averaging time. All ramp-up events fell within the bounds of the SBL at the

suggested 15 s - 60 s averaging times. However, exceedances greater than the 60 s averaging time and high variability at all averaging times illustrates the non-stationarity of these events and possibly uncaptured turbulence regimes.

Acknowledegments

Jeff Livingston, Glenn Allen, Brad Coffman and George Riddick are acknowledged for their service at the Texas Tech University field site. Dr. Chris Weiss, Brian Hirth, Wesley Burgett, Pat Skinner and Jason McNeill asssited with some of the data acquistion. Thanks are extended to Kelsey Seger and Carol Ann Stanley of the Wind Science and Engineering department at Texas Tech for their logisitical and administrative support.

F.T. Lombardo finalized this work during his current tenure as a NIST/NRC Postdoctoral Research Associate. National Science Foundation (Grant No. 0221688) provided part of the funding for this research through support of F.T. Lombardo while a graduate student at Texas Tech University. Dr. Andy Swift of Texas Tech is also acknowledged for funding support provided through the Texas Wind Energy Institute.

References

American Society of Civil Engineers (ASCE). (2010). *Minimum design loads for buildings and other structures, ASCE/SEI 7-10*, Reston, VA.

Bendat, J.S., and Piersol, A.G. (2000). *Random data analysis and measurement procedures*, Wiley-Interscience, New York, 594 pp.

Chay, M.T., Wilson, R., and Albermani, F. (2008). "Gust occurrence in simulated non-stationary winds", *J. Wind Eng. Ind. Aerodyn.*, **96**, 2161-2172

Chen, L., and Letchford, C.W. (2005). "Proper orthogonal decomposition of two vertical profiles of full-scale nonstationary downburst wind speeds", *J. Wind Eng. Ind. Aerodyn.*, **93**, 187-216

Chen, L., and Letchford, C.W. (2007). "Numerical simulation of extreme winds from thunderstorm downbursts", *J. Wind Eng. Ind. Aerodyn.*, **95**, 977-990

Choi, E.C.C. (2000). "Wind characteristics of tropical thunderstorms", *J. Wind Eng. Ind. Aerodyn.*, **84**, 215-226

Choi, E.C.C. (2004). "Field measurement and experimental study of wind speed profiles during thunderstorms", *J. Wind Eng. Ind. Aerodyn.*, **92**, 275-290

Choi, E.C.C., and Hidayat, F. A. (2002). "Gust factors for thunderstorm and non-thunderstorm winds", *J. Wind Eng. Ind. Aerodyn.*, **90**, 1683-1696

Duranona, V., Sterling, M., Baker, C.J. (2007). "An analysis of extreme non-synoptic winds", *J. Wind Eng. Ind. Aerodyn.*, **95**, 1007-1027

Ewing, B.T., Kruse, J.B., and Schroeder, J.L. (2005). "Time series analysis of wind speed with time-varying turbulence", *Environmetrics*, **17**, 119-127

Fujita, T.T. (1981). “Tornadoes and downbursts in the context of generalized planetary scales”, *J. Atmo. Sci.*, **1981**, 1511-1534

Fujita, T. (1985). *The Downburst*, SMRP 210, U. of Chicago Press

Fujita, T. (1986). *DFW Microburst*, SMRP 217, U. of Chicago Press

Gurley, K.M., Kijewski, T., and Kareem, A. (2003). “First- and higher-order correlation detection using wavelet transforms”, *J. Eng. Mech.*, **129**, 188-201

Hjelmfelt M. R. (1988). “Structure and life cycle of microburst outflows observed in Colorado.” *J. App. Meteo.*, **27**, 900-927.

Holmes, J.D. (2001). *Wind Loading on Structures*. Spon Press, London-NY

Holmes, J. D., and Oliver, S. E. (2000). “An empirical model of a downburst.” *Eng. Struct.*, **22**, 1167-1172.

Holmes, J.D., Hangan, H.M., Schroeder, J.L., Letchford, C.W., Orwig, K.D. (2008). “A forensic study of the Lubbock-Reese downdraft of 2002”, *Wind and Structures*, **11**, 137-152

Juhásová, E. (1997), “Quasi-static versus dynamic space wind response of slender structures”, *J. Wind Eng. Ind. Aerodyn.*, **69-71**, 757-766

Kim, J. and Hangan, H. (2007). “Numerical simulations of impinging jets with application to downbursts”, *J. Wind Eng. Ind. Aerodyn.*, **95**, 4, 279-298

Kwon, D. and Kareem, A. (2009). “Gust front factor: New framework for wind load effects on structures”, *J. Struct. Eng.*, **135**, 6, 717-732

Levitan, M. and Mehta, K.C. (1992). “Texas Tech field experiments for wind loads part II: meteorological instrumentation and terrain parameters”, *J. Wind Eng. Ind. Aerodyn.*, **41-44**, 1577-1588

Li, C.Q. (2000). "A stochastic model of severe thunderstorm for transmission line design", *Prob. Eng. Mech.*, **15**, 359-364

Lombardo, F.T. (2009). *Analysis and Interpretation of Thunderstorm Wind Flow on a Bluff Body*, Ph.D. Dissertation, Texas Tech University, 259 pp.

Mason, M.S., Letchford, C.W., James, D.L. (2005). "Pulsed wall jet simulation of a stationary thunderstorm downburst, Part A: Physical structure and flow field visualization", *J. Wind Eng. Ind. Aerodyn.*, **93**, 557-580

Masters, F. J. (2004). *Measurement, modeling and simulation of ground-level tropical cyclone winds*, Ph.D. Dissertation, University of Florida, 189 pp.

National Institute of Standards and Technology (NIST, 2006). "Trend Tests", http://www.itl.nist.gov/div898/handbook/apr/section2/apr234.htm (Accessed May 1, 2009)

Orwig, K.D. and Schroeder, J.L. (2007). “Near surface wind characteristics of extreme thunderstorm outflows”, *J. Wind Eng. Ind. Aerodyn.*, **95**, 565-58

Percival, D.B. and Walden, A.T. (2000). *Wavelet Methods for Time Series Analysis*, Cambridge University Press

Ponte, J. and Riera, J.D. (2007). "Wind velocity field during thunderstorms", *Wind and Structures*, **10**, 287-300

Ponte, J. and Riera, J.D. (2010). "Simulation of extreme wind series caused by thunderstorms in temperature latitudes", *Struct. Safety*, **32**, 231-237

Schroeder, J.L, Burgett, W.S., Haynie, K.B., Sonmez, I., Skwira, G.D., Doggett, A.L. and Lipe, J.W. (2005). "The West Texas mesonet: A technical overview", *J. Atmos. Ocean. Tech.*, **22**, 211-222

Schroeder, J.L., Weiss, C.C. and Guynes, J.G. (2009). "Innovative technologies to investigate fine scale atmospheric motions and their impact", *Proc. 11th Americas Conference on Wind Engineering, San Juan, PR*, CD-ROM

Simiu, E. and Miyata, T. (2006). *Design of Buildings and Bridges for Wind*, Wiley, 308 pp.

Simiu, E. and Scalan R.H. (1986). *Wind Effects on Structures*, Wiley, 688 pp.

Skinner, P.S., Weiss, C.C., Reinhart, A.E., Gunter, W.S., Schroeder, J.L., Guynes, J. (2010). "TTUKa mobile Doppler radar observations of near-surface circulations in VORTEX2", *Proc. 25th Conf. on Severe Local Storms*, Denver, CO

Stull, R.B. (1988). *An Introduction to Boundary Layer Meteorology*, Kluwer, 666 pp.

Vega R. (2008). *Wind directionality: A reliability based approach*, Ph.D. Dissertation, Texas Tech University, 303 pp.

Wakimoto, R. (2001). "Convectively driven high wind events" *Severe Convective Storms*, Dowsell, C. ed.

Wang L. and Kareem, A. (2005). "Modeling and simulation of transient winds in downbursts/hurricanes" *Proc. 10th Americas Conf. on Wind Engineering*, Baton Rouge, LA

Wood, G.S., Kwok, C.S., Motteram, N.A., Fletcher, D.F. (2001), "Physical and numerical modelling of thunderstorm downbursts", *J. Wind Eng. Ind. Aerodyn.*, **89**, 535–552.

Tables

Table 1. Summary of ramp-up thunderstorm events.

Date	Measured	Storm Type	Temporal Scale (s)	Peak Wind (mph)	Profile
June 19, 2003	160 ft Tower	Non-Supercell	100	~60	Yes
May 20, 2006	200 m Tower	Non-Supercell	200	~60	No
May 14, 2008	StickNet	Supercell	250	~80	No
May 21, 2008	200 m Tower	Non-Supercell	170	~70	Yes
June 19, 2008	200 m Tower	Non-Supercell	75	~60	Yes
August 14, 2008	200 m Tower	Non-Supercell	150	~60	Yes
June 4, 2009	200 m Tower	Bow Echo/Supercell	300	~80	Yes
August 12, 2009	200 m Tower	Non-Supercell	75	~60	Yes

Table 2. The averaging times, *t*, used in the computation of residual turbulence

Number	*t(s)*	*Number*	*t(s)*
1	1.1	11	34.1
2	1.6	12	51.2
3	2.1	13	68.3
4	3.2	14	102.4
5	4.3	15	136.5
6	6.4	16	204.8
7	8.5	17	273.1
8	12.8	18	409.6
9	17.1	19	546.1
10	25.6	20	723

Figure Captions

Fig. 1. Illustration of a statistically stationary wind event (left) and a non-stationary thunderstorm wind event (right) at 10 m (33 ft).

Fig. 2. Time histories of the eight ramp-up events described in Table 1. Order is the same as Table 1 from left to right.

Fig. 3. Thunderstorm time histories displaying periodic components.

Fig. 4. Comparison of periodic thunderstorm events with SBL.

Fig. 5. Two VORTEX cases displaying low frequency, periodic characteristics.

Fig. 6. Varying residual turbulence from thunderstorm event using an averaging time of 34 s.

Fig. 7. Thunderstorm wind speed time history (black, left), the 17 s moving average (gray, left) and the residual turbulence (right). Change points indicated as gray vertical dashed lines. Residual turbulence segment is taken between the two change points containing the maximum.

Fig. 8. Mean residual turbulence of thunderstorm events. Ramp-up events in gray.

Fig. 9. Ramp-up composite spectra compared to SBL models.

Fig. 10, 11. Wavelet analysis for ramp-up cases on June 19, 2003 and June 4, 2009 respectively.

Fig. 12. Effect of avergaing time on SBL turbulence intensity values.

Fig. 13. Turbulence intensity values of ramp-up and range of SBL events.

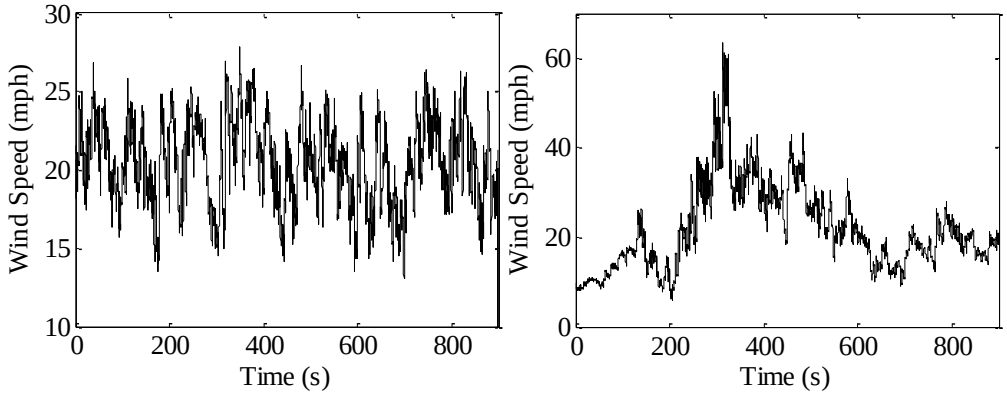
30
25
20
15
10
Wind Speed (mph)
0
200
400
600
800
Time (s)
60
40
20
0
Wind Speed (mph)
0
200
400
600
800
Time (s)

Figure 1

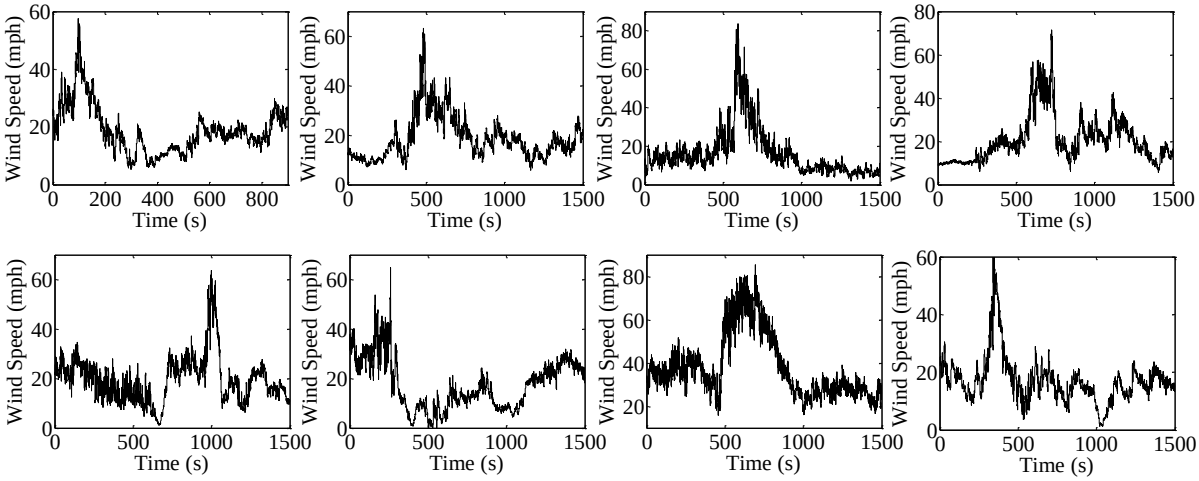

Figure 2

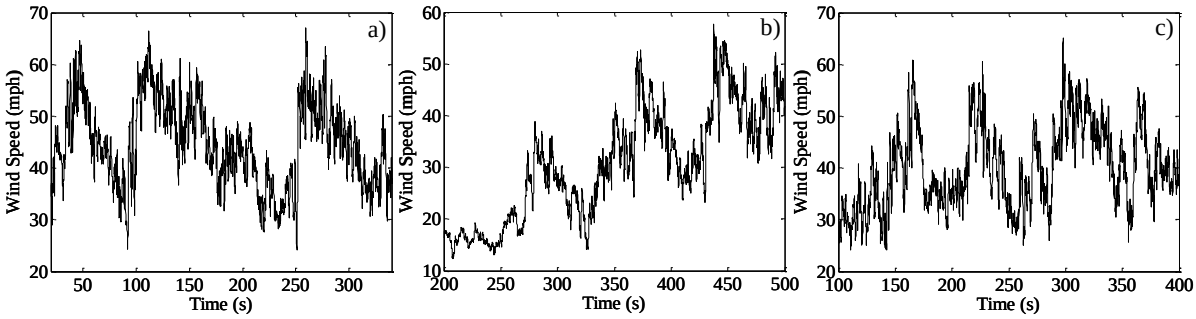
a)
b)
c)
Wind Speed (mph)
Time (s)
70
60
50
40
30
20
10
50
100
150
200
250
300
350
400
450
500

Figure 3

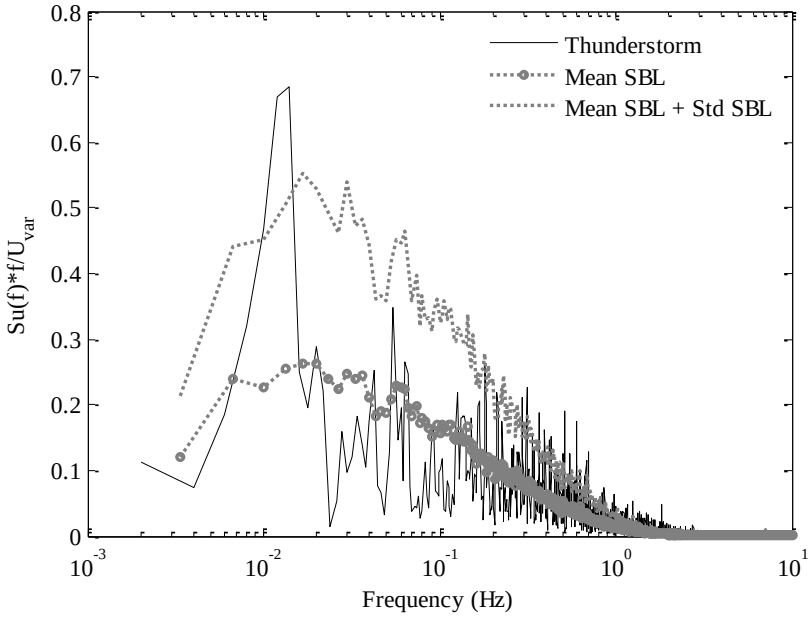
Thunderstorm
Mean SBL
Mean SBL + Std SBL
Su(f)*f/U_var
Frequency (Hz)
0.8
0.7
0.6
0.5
0.4
0.3
0.2
0.1
0
10^-3
10^-2
10^-1
10^0
10^1

Figure 4

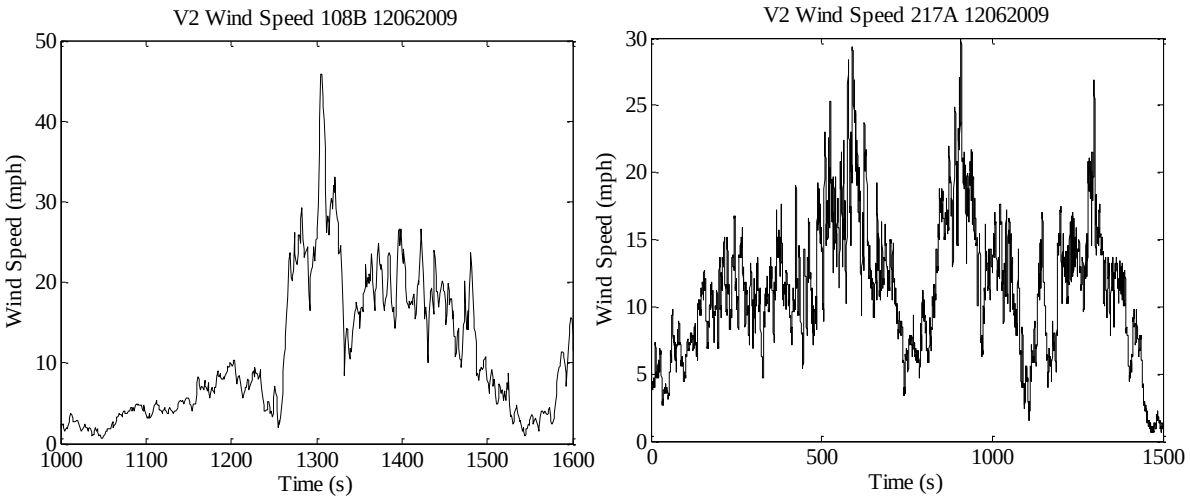
V2 Wind Speed 108B 12062009
Wind Speed (mph)
Time (s)
0
10
20
30
40
50
1000
1100
1200
1300
1400
1500
1600
V2 Wind Speed 217A 12062009
Wind Speed (mph)
Time (s)
0
5
10
15
20
25
30
0
500
1000
1500

Figure 5

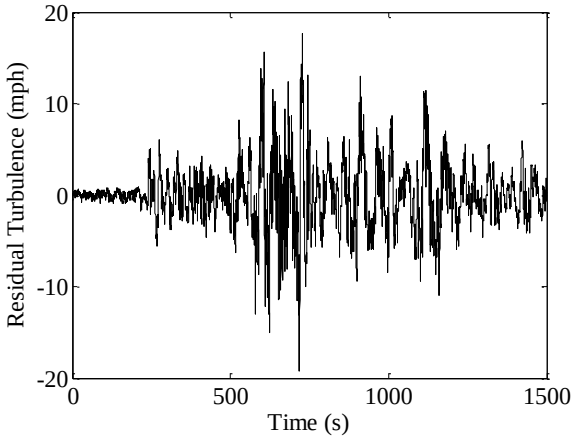

Figure 6

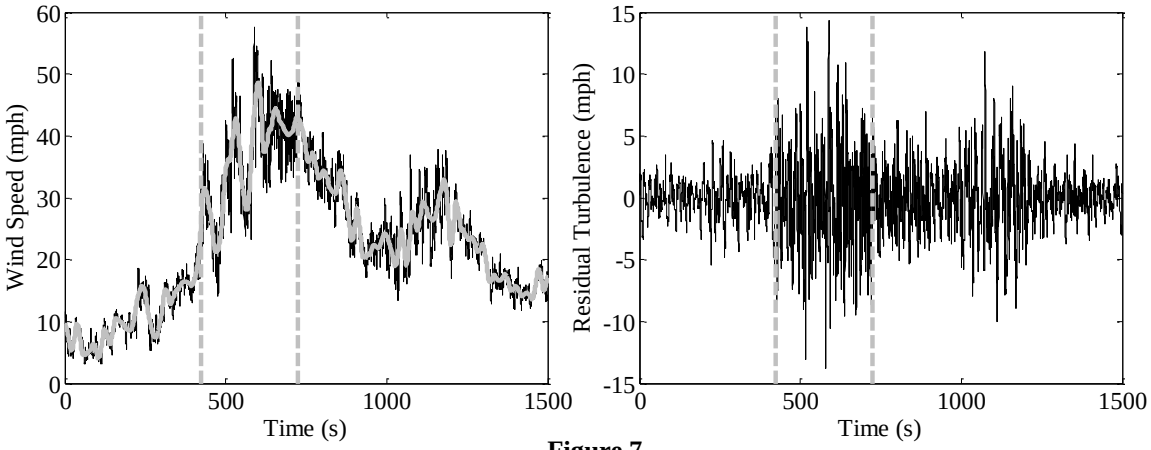

Figure 7

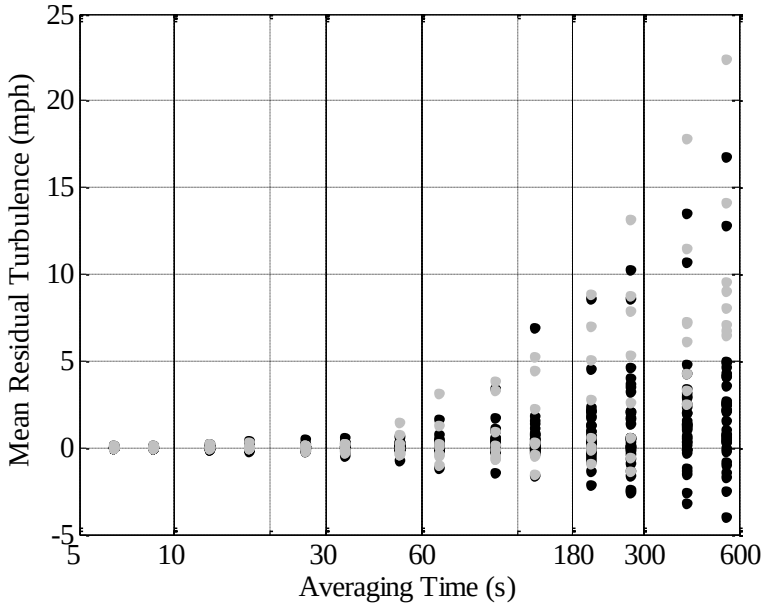
25
20
15
10
5
0
-5
Mean Residual Turbulence (mph)
5
10
30
60
180
300
600
Averaging Time (s)

Figure 8

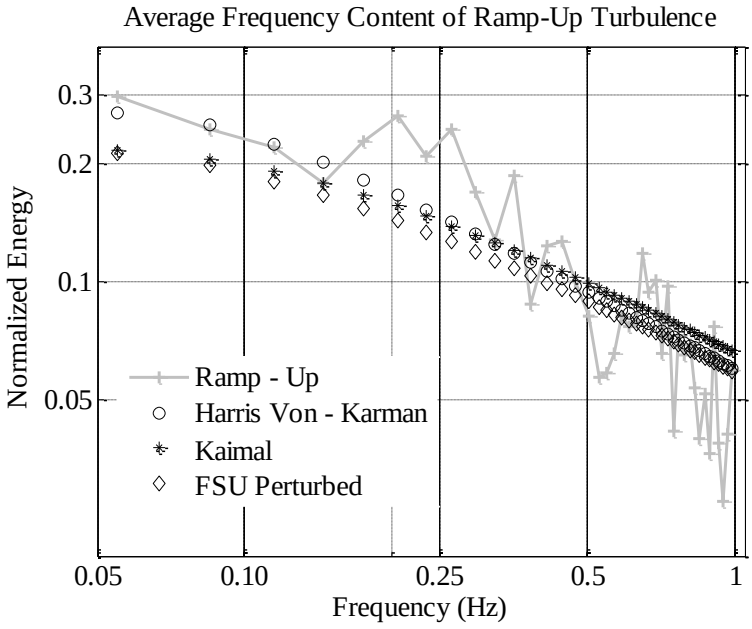
Average Frequency Content of Ramp-Up Turbulence
Normalized Energy
0.3
0.2
0.1
0.05
Ramp - Up
Harris Von - Karman
Kaimal
FSU Perturbed
0.05
0.10
0.25
0.5
1
Frequency (Hz)

Figure 9

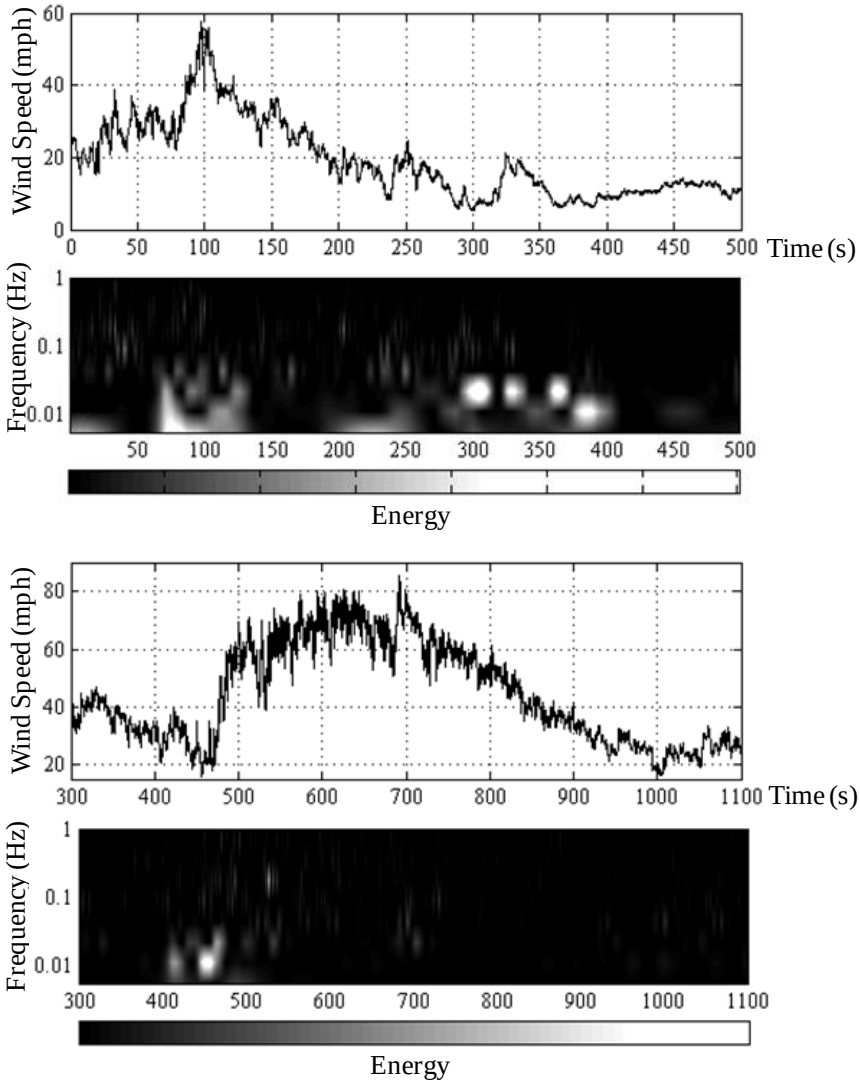

Figures 10 and 11

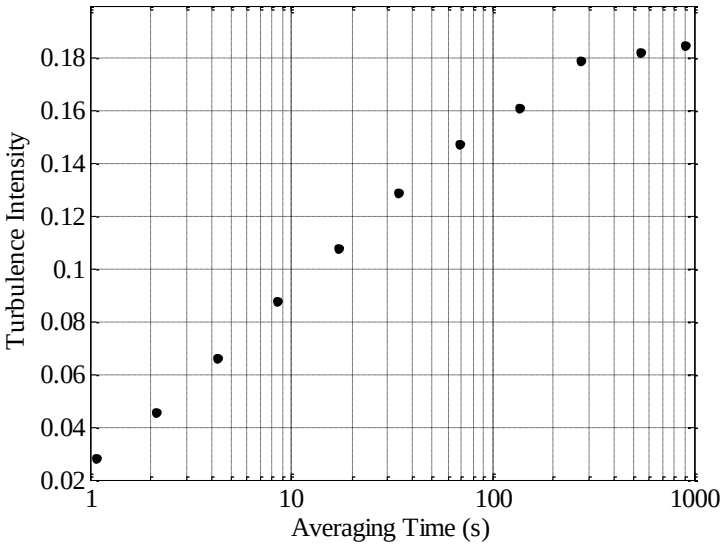
Turbulence Intensity
0.18
0.16
0.14
0.12
0.1
0.08
0.06
0.04
0.02
1
10
100
1000
Averaging Time (s)

Figure 12

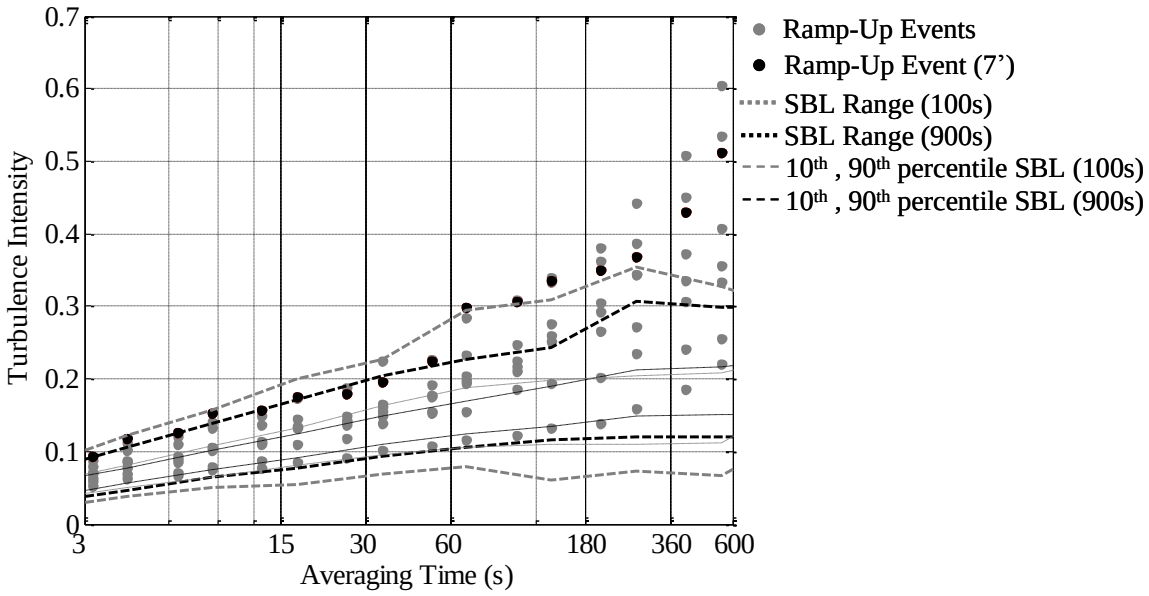
0.7
0.6
0.5
0.4
0.3
0.2
0.1
0
Turbulence Intensity
3
15
30
60
180
360
600
Averaging Time (s)
Ramp-Up Events
Ramp-Up Event (7')
SBL Range (100s)
SBL Range (900s)
10th , 90th percentile SBL (100s)
10th , 90th percentile SBL (900s)

Figure 13